

MAGNETOELECTRIC COUPLING OF BI-LAYER AND TRI-LAYER (2-2) LSMO/P(VDF-TrFE) LAMINATE COMPOSITE AT ROOM TEMPERATURE

Sougata Koner^{1,3}, Sumit^{2,3}, R. Shukla^{2,3}, S. K. Majumder^{1,3} and S. Satapathy^{1,3}

¹Laser Biomedical Applications Division, Raja Ramanna Centre for Advanced Technology, Indore, 452013, India

²Accelerator Physics and Synchrotrons Utilization Division, Raja Ramanna Centre for Advanced Technology, Indore, 452013, India

³Homi Bhabha National Institute, Training School Complex, Anushakti Nagar, Mumbai-400094, India

ABSTRACT

Bilayer and Tri-layered laminated composites of (2-2) LSMO/P(VDF-TrFE) are prepared using adhesive method. Tri-layer structure shows the higher magnetoelectric (ME) coupling coefficient with higher bias magnetic field compared to the bi-layer structure. Finite element method (FEM) based simulation for ME using COMSOL Multiphysics 6.0 software for the bi-layer and the tri-layer structure supports the experimental findings. Both the experimental and simulation determination confirms the strain mediated ME effect in the bilayer and tri-layer laminated LSMO/P(VDF-TrFE) structures.

KEYWORDS

Polymer composite, magnetostriction, magnetoelectric effect, laminate structure.

1. INTRODUCTION

Magneto Electric (ME) coupling coefficient of composites depends upon the fabrication methods and connectivity like particulate i. e. (0-3) connectivity, fiber/rod like i.e. (1-3) connectivity, laminate i. e. (2-2) connectivity [1]. In case of (0-3) structure, the ME coefficient is quite small, as the stress induced in the piezoelectric phase is not large. Agglomeration of the piezomagnetic nanoparticles in piezoelectric matrix makes electric poling difficult due to large conductivity of the piezomagnetic phase and leakage of charges which reduces the number of interfaces, whereas in (1-3) structure the ordering of the piezomagnetic phase is higher as compared to (0-3) structure which enhances the strain transfer but still there is leakage of charges [2]. On the other hand (2-2) structure carries many advantages over other structures like: large interfacial coupling interface enhances strain transfer between layers and minimizes leakage of charges due to piezoelectric layer having very less conductivity which enhances the electric poling condition of structure [1,2]. Manganite materials (based on composition dependent of the phase diagram) show excellent magnetostriction and double exchange mediated ferromagnetism at room temperature [3, 4, 5, 6, 7]. Among the ferromagnetic manganite compounds, $\text{La}_{0.7}\text{Sr}_{0.3}\text{MnO}_3$ (LSMO) has largest volume magnetostriction ($\sim 10^{-4}$), highest Curie temperature $\sim 370\text{K}$ with colossal magnetoresistance (CMR) properties [8, 9]. Studies on the ME coupling effect in (0-3) nanocomposite (NC) films of LSMO/P(VDF-TrFE) shows that this composite exhibits a maximum ME coupling coefficient of 155.74 mV/Oe-cm [10]. Earlier, we have reported ME coupling coefficient for bi-layer (2-2) LSMO/P(VDF-TrFE) prepared by adhesive method which

shows a maximum of 16.88 mV/Oe-cm (Experimental value) and 14.32 mV/Oe-cm (Simulated value) [2]; however, these reported values are small compared to (0-3) composites which in general should not be. So, in this manuscript we have reported the ME coefficient of (2-2) LSMO/P(VDF-TrFE) prepared by taking the epoxy layer in between LSMO and P(VDF-TrFE) layers as well as developed the Finite element method (FEM) based simulation model. In this manuscript, the magnetoelectric effect of (2-2) LSMO/P(VDF-TrFE) composite in the form of bilayer (P-M) and tri-layer or sandwiched (P-M-P) structures are explored taking consideration of the following matters: the laminate composite was prepared by keeping the aspect ratio of the P(VDF-TrFE) and LSMO layer same (4mm×4mm) to increase the magnetostriction effect and also to measure physically the ME coupling coefficient [11,2]; the thickness of the P(VDF-TrFE) layer is kept 30µm for the effective transmission of the strain through the interface and to minimize the effect of in homogeneous strain distribution [12]; the thickness of the LSMO layer is kept 0.3 mm to reduce the required bias magnetic field, to decrease the brittleness of the composite, to reduce the eddy current effect and also to reduce the leakage of charges; the epoxy layer used to adhesion the LSMO and P(VDF-TrFE) layers is kept as thin as possible to transfer the strain through the interfaces easily [12]. The bilayer (P-M) and tri-layer or sandwich (P-M-P) structure were fabricated for ME coupling study whereas the (M-P-M) structure is neglected as this structure is more brittle and higher DC bias magnetic field is required for study. Further, FEM based model is developed in the COMSOL Multiphysics 6.0 software for the determination of the ME coupling coefficient (α_H^V) for the bi-layer (P-M) and tri-layer (P-M-P) structures. Finally simulated result is compared with the experimental results.

2. EXPERIMENT DETAILS

2.1. Experimental technique and FEM based ME simulation model

LSMO nano particles is synthesized by sol gel auto combustion method [10]. P(VDF-TrFE) films were prepared by solution casting method [2]. The P-M and P-M-P type LSMO/P(VDF-TrFE) laminate composites was fabricated by adhesion of LSMO pellet (4mm×4mm×0.3mm) and P(VDF-TrFE) films (4mm×4mm×0.03mm) using epoxy. The schematic diagrams for the P-M and P-M-P structures are shown in the Fig. 1. The polarization of each P(VDF-TrFE) layer in the P-M and P-M-P structure is directed perpendicular of film surface by application of electric voltage of 1kV. The pre-requisite magnetic bias field is applied parallel to the laminate composite's surface to align magnetization of LSMO layer.

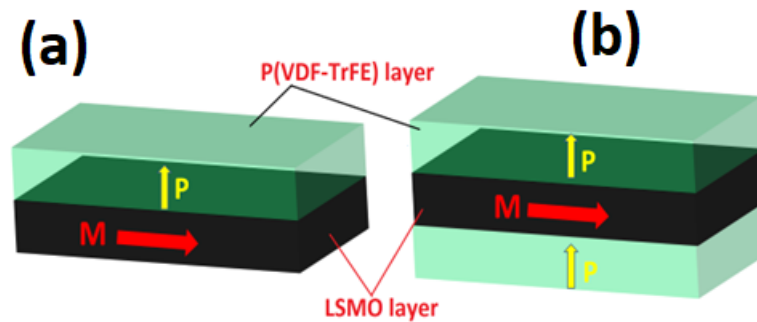


Figure 1. Schematic diagram of (a) bilayer (P-M) and (b) tri-layer (P-M-P) structure

ME coupling measurement was performed by Lock-in technique and ME voltage was measured along the thickness direction (31-mode) of the bi-layer and tri-layer structures. The Schematic diagram of the ME coupling set-up is shown in the Fig.2(a). The DC magnetic field and AC

magnetic field are applied to samples by the Electromagnets and the Helmholtz coils respectively (Shown in Fig. 2(b)). The ME voltage is measured by the Lock-in amplifier at the reference frequency fed up by the function generator. A power amplifier is used to properly capture (amplify) the ME signal from the samples and send it to in the lock-in amplifier. Room temperature XRD pattern of P(VDF-TrFE) film, LSMO NPs and LSMO pellet have been done using Rigaku Geigerflex (Cu $K\alpha$ radiation $\lambda=1.5406\text{\AA}$) diffractometer. The magnetostriction(λ) of the LSMO layer is measured by the strain gauge technique. Room temperature magnetization(M) Vs. applied magnetic field(H) hysteresis is traced by S700X SQUID magnetometer.

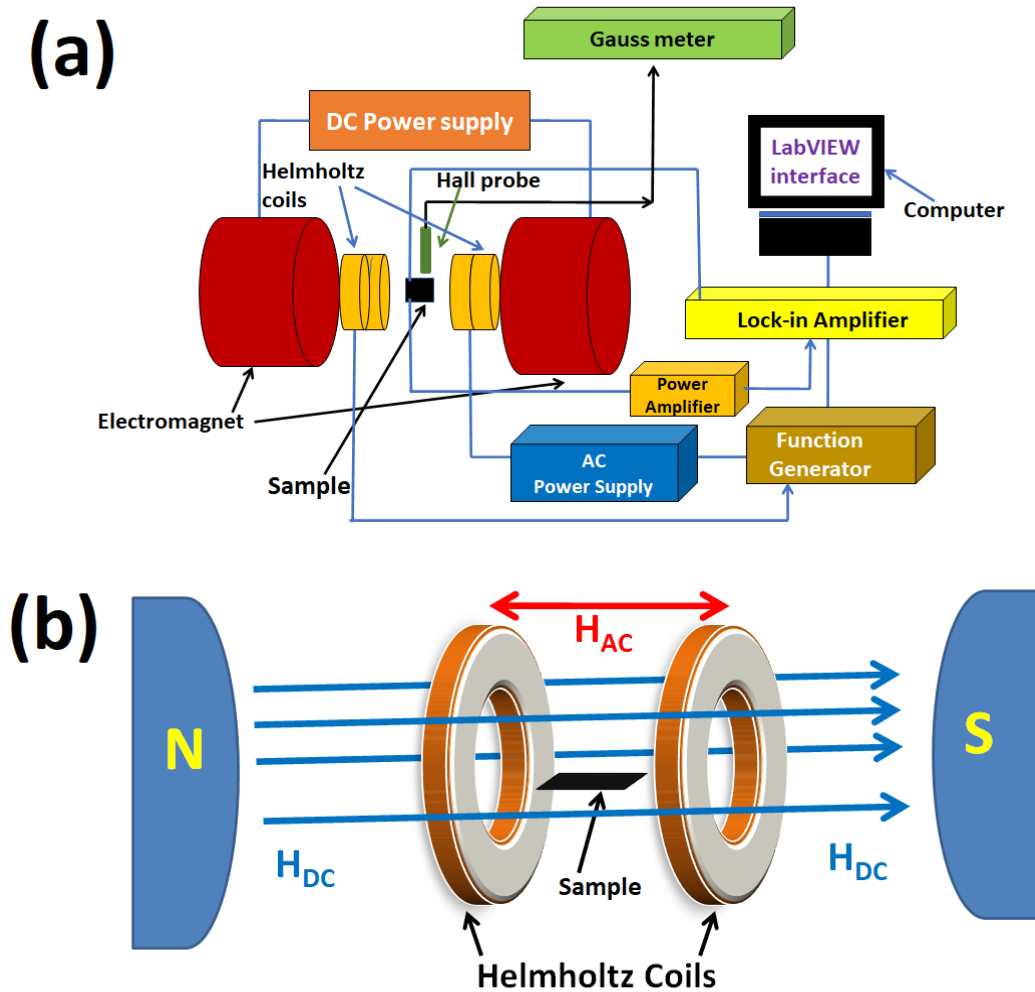


Figure 2. (a)Lock-in technique for the ME coupling coefficient measurement; (b)magnetic field directions in the sample position

Finite element method (FEM) was also performed for the estimation of ME coefficient of LSMO/P(VDF-TrFE) bilayer (P-M) and tri-layer or sandwiched (P-M-P) composite. The developed coupled FEM based model in COMSOL Multiphysics 6.0 software and the assumptions for the modelling were described earlier [2]. In this model, “Solid mechanics”, “Electrostatic” and “Magnetic field” physics as well as “Piezoelectric effect” and “Magnetostriction” Multiphysics were used in FEM modeling of laminated bi-layer and tri-layer LSMO/P(VDF-TrFE) composite (Shown in Fig. 3). Magneto-striction effect in the LSMO layer

was modeled by non-linear isotropic model [2]. Piezoelectric effect in P(VDF-TrFE) was modeled by linear constitutive equation of piezoelectricity [2].

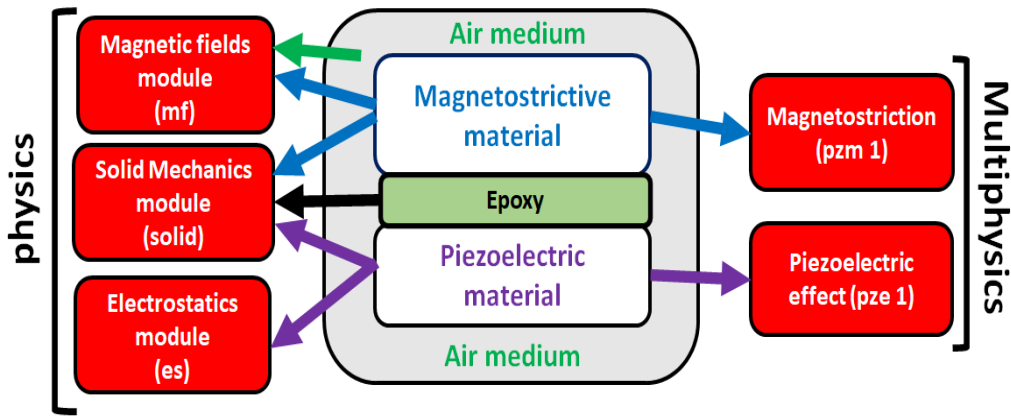


Figure 3. Modules and Multiphysics used in the COMSOL simulation

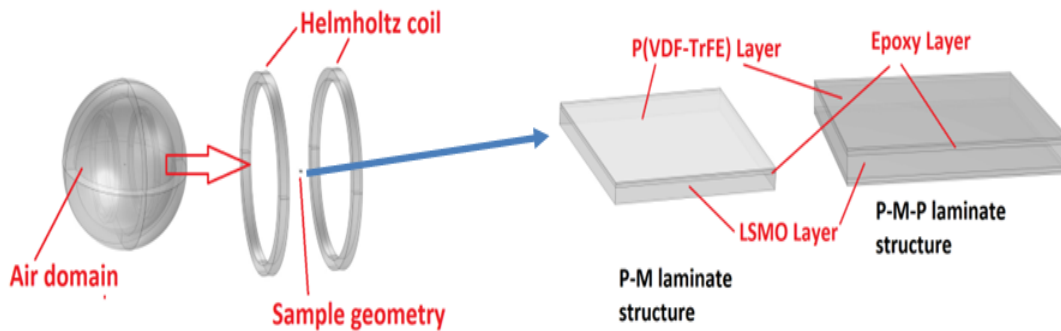


Figure 4. Geometry of the FEM based model in COMSOL Multiphysics 6.0 software and the structure of the P-M and P-M-P composites

Geometry of the FEM based ME model set up in COMSOL Multiphysics 6.0 software and the structure incorporating the layers of LSMO, P(VDF-TrFE) and epoxy for the P-M and P-M-P composite are shown in the Fig. 4. In the COMSOL Multiphysics 6.0 FEM model set up, an AC magnetic field was applied using a pair of Helmholtz coils along. A collinear DC biasing magnetic field was applied with parametric sweep in the range (0-5) kOe. To solve the developed FEM model, “Small signal analysis” study was used [2,13]. An infinite air domain is considered in the modelling to accurately capture the behaviour of bilayer (P-M) and sandwiched (P-M-P) LSMO/P(VDF-TrFE) composite in magnetic field [2,13].

2.2. Equations for the FEM based ME modelling in COMSOL 6.0 Multiphysics

Applied magnetic field (H) produces magnetostriction (λ) in the LSMO layer by changing the shape of the LSMO layer with rotation of magnetization (M), M is modelled by the Nonlinear isotropic model and Langevin function as [14,15]:

$$M = M_s L\left(\frac{|H_{eff}|}{M_s}\right) \frac{H_{eff}}{|H_{eff}|} \dots\dots\dots (1)$$

$$L = \coth\left(\frac{3\chi_m |H_{eff}|}{M_s}\right) - \frac{M_s}{3\chi_m |H_{eff}|} \dots\dots\dots (2)$$

$$H_{eff} = H + \frac{3\lambda_s}{\mu_0 M_s^2} \sigma_{dev} M \dots\dots\dots (3)$$

$$B = \mu_0 (H + M) \dots\dots\dots (4)$$

where H_{eff} is the effective magnetic field; λ_s is the saturation magnetostriction corresponding to saturation magnetization (M_s); χ_m is the magnetic susceptibility of the magnetic material, μ_0 is the magnetic permeability; σ_{dev} is the deviatoric stress tensor; B is the magnetic induction intensity and H is the magnetic field intensity.

The magnetostrictive strain (ε_H^m) is expressed as [14,15]:

$$\varepsilon_H^m = \frac{3}{2} \frac{\lambda_s}{M_s^2} dev(M \otimes M) \dots\dots\dots (5)$$

where, $dev(M \otimes M) = M_i M_j$ i. e. represents the deviatoric tensors of M.

The stress tensor (σ^m) with the applied H is related to the strain tensor as [15]:

$$\sigma^m - \sigma_0^m = C_E^m (\varepsilon^m - \varepsilon_H^m) \dots\dots\dots (6)$$

where, σ_0^m is the initial stress tensor and ε^m is the initial strain tensor; C_E^m is the elastic matrix which is a function of Young's modulus (Y) and Poisson's ratio (σ).

The strain generated in the LSMO layer by H passes to the P(VDF-TrFE) layer which produces the output electric voltage. The strain and output electric voltage in the P(VDF-TrFE) layer is modelled by the equations of the piezoelectric effect [14,15]:

$$\varepsilon^p = S^E \sigma^p + d^T E \dots\dots\dots (7)$$

$$D = d \sigma^p + \epsilon E \dots\dots\dots (8)$$

where ε^p is the strain tensor; S^E is the compliance tensor; d is the piezoelectric coefficient tensor; D is the electric displacement tensor, E is the electric field tensor and ϵ is the permittivity tensor of the piezoelectric material. The parameters and the value used in the ME effect modelling in COMSOL Multiphysics 6.0 software for the P(VDF-TrFE) layer, LSMO layer and epoxy layer are listed in Table 1, Table 2 and Table 3 respectively.

Table 1. Parameters value used in the FEM modelling for P(VDF-TrFE) layer

Property	Parameter value
Density	1850 Kg/m ³
Compliance matrix (S^E)	$\begin{bmatrix} 3.32 & -1.44 & -0.89 & 0 & 0 & 0 \\ & 3.34 & -0.86 & 0 & 0 & 0 \\ & & 3 & 0 & 0 & 0 \\ & & & 94 & 0 & 0 \\ & & & & 96.3 & 0 \\ & & & & & 14.4 \end{bmatrix} \times 10^{-10} \frac{m^2}{N}$
Coupling matrix(d)	$\begin{bmatrix} 0 & 0 & 0 & 0 & -36.3 & 0 \\ 0 & 0 & 0 & -40.6 & 0 & 0 \\ 10.7 & 10.1 & -33.5 & 0 & 0 & 0 \end{bmatrix} \times 10^{-12} \frac{C}{N}$
Relative permittivity matrix(ϵ)	$\begin{bmatrix} 7.4 & 0 & 0 \\ 0 & 7.95 & 0 \\ 0 & 0 & 7.9 \end{bmatrix}$

Table 2. Parameters value used in the FEM modelling for LSMO layer

Property	Parameter value
Young Modulus	113GPa
Poisson's ratio	0.36
Density	6450 Kg/m ³
Saturation magnetostriction	20 ppm

Table 3. Parameters value used in the FEM modelling for epoxy layer

Property	Parameter value
Density	1400 Kg/m ³
Young Modulus	1.85GPa
Poisson's ratio	0.33

3. RESULTS AND DISCUSSION

Room temperature XRD pattern of the P(VDF-TrFE) film is shown in the Fig. 5(a), which shows the existence of the (110)/(200) characteristic β -peak of P(VDF-TrFE); hence polar P(VDF-TrFE) phase has been formed. The XRD- pattern of the LSMO NPs and LSMO pellet also have been shown in the Fig.5(a) which shows the phase formation in accordance of JCPDS card no. 00-051-0409. Fig. 5(b) shows the room temperature of (M Vs. H) hysteresis plot of LSMO pellet,

this plot shows the ferromagnetic nature of the LSMO layer with saturation magnetization (M_s) \sim 4 emu/g with very low coercivity (\sim 10 Oe). The M^2 -H plot at the room temperature for LSMO layer

is shown in Fig. 5(c). Since, there is a proportionality relation between magnetostriction (λ) and M^2 , the information of magnetostriction (λ) can be explored from this plot. It may be predicted that, λ increases up to M_s with the increase of M then it saturates. The variation of dM^2/dH with H for LSMO layer is shown in Fig. 5(d). Since, α_H^V is proportional to dM^2/dH or $d\lambda/dH$, this plot (Fig. 5(d)) shows the correlation of dM^2/dH with α_H^V . This correlation signifies that, α_H^V increases up to a value where $d\lambda/dH$ maximizes or maximum strain transferred, then α_H^V falls with increase in H [16]. Fig. 5(e) shows the variation of in-plane magnetostriction of LSMO pellet with the H , it is observed that, with the increase in H , in-plane magnetostriction increases and attains a saturation value \sim 20 ppm. The corresponding piezomagnetic coefficient ($q = \frac{d\lambda}{dH}$) [16,10] for the LSMO pellet is also shown in the Fig.5(e), which is found to be $q=0.033$ ppm/Oe.

The variation of experimental α_H^V (in 31-mode) in the response to the in-plane applied H_{DC} for tri-layer (P-M-P) and bilayer (P-M) LSMO-P(VDF-TrFE) laminated structure are shown in Fig. 6 (a) and Fig. 6 (b) respectively. The variation of FEM simulated α_H^V (in 31-mode) with H_{DC} for tri-layer (P-M-P) and bilayer (P-M) LSMO-P(VDF-TrFE) laminated composites are shown in Fig. 6(c). Both experimental and simulated α_H^V increases with H_{DC} and attains maximum amplitude at a certain optimum field of H_{DC} ($H_{DC, OPT.}$) and then decreases non-linearly with further increase of H_{DC} . The experimental and simulated α_H^V values for P-M-P and P-M structures differ in magnitude and point of origin. The experimental and simulated α_H^V values for both the structures are tabulated in the Table 4. Tri-layer(P-M-P) composite is showing higher α_H^V compared to the bi-layer(P-M) structure and the required bias field is also higher in P-M-P structure compared to P-M structure.

When H_{DC} is applied in in-plane direction, the magnetic moments of the LSMO layer rotates and gets aligned in the field direction by joule magnetostriction (λ) [17,10]. Above a certain optimum field of H_{DC} , λ saturates for higher field above H_{DC} . As a result, the rate of change of λ with H diminishes which diminishes the response of magnetic moments with the H [16,10]. The generated strain in LSMO layer is passed to the elastically coupled P(VDF-TrFE) layer, which changes the polarizations of the electric dipoles of P(VDF-TrFE) along the thickness of the P(VDF-TrFE) layer [10,16,17]. Thus, ME voltage is produced in the P(VDF-TrFE) layers are along the thickness of the P-M and P-M-P structures. The higher ME voltage generated in the tri-layer structure may be explained as: two P(VDF-TrFE)-LSMO interfaces in the P-M-P structure transfers higher interfacial strain than the strain passed through the single layer in the P-M or bilayer structure [18]. The requirement of higher magnetic bias magnetic field in the tri-layer structure can be explained as: two epoxy layer present in the P-M-P structure constrained the magnetostriction produced by the LSMO layer; so, to produce the same amount of magnetostriction as compared to P-M structure higher bias magnetic field is required in the P-M-P structure [19].

The deviation in the starting point of experimental and simulated results is mainly due to the assumptions of zero the remnant polarization in P(VDF-TrFE) phase and remnant magnetization in LSMO phase during simulation. In experiment, the output voltage obtained only when LSMO layer is magnetically poled and P(VDF-TrFE) layer is electrically poled. So, the sample is already in remnant magnetization and remnant polarization state. This is the reason why the simulated curve started from origin and experimental curve starts from finite value. The deviation in magnitude in the simulated and experimental α_H^V may be attributed to limitation software to incorporate remnant magnetization and polarization in the modelling and use of power amplifier

the ME coupling experimental set up (shown in the Fig. 2(a)) which may amplifies the ME voltage.

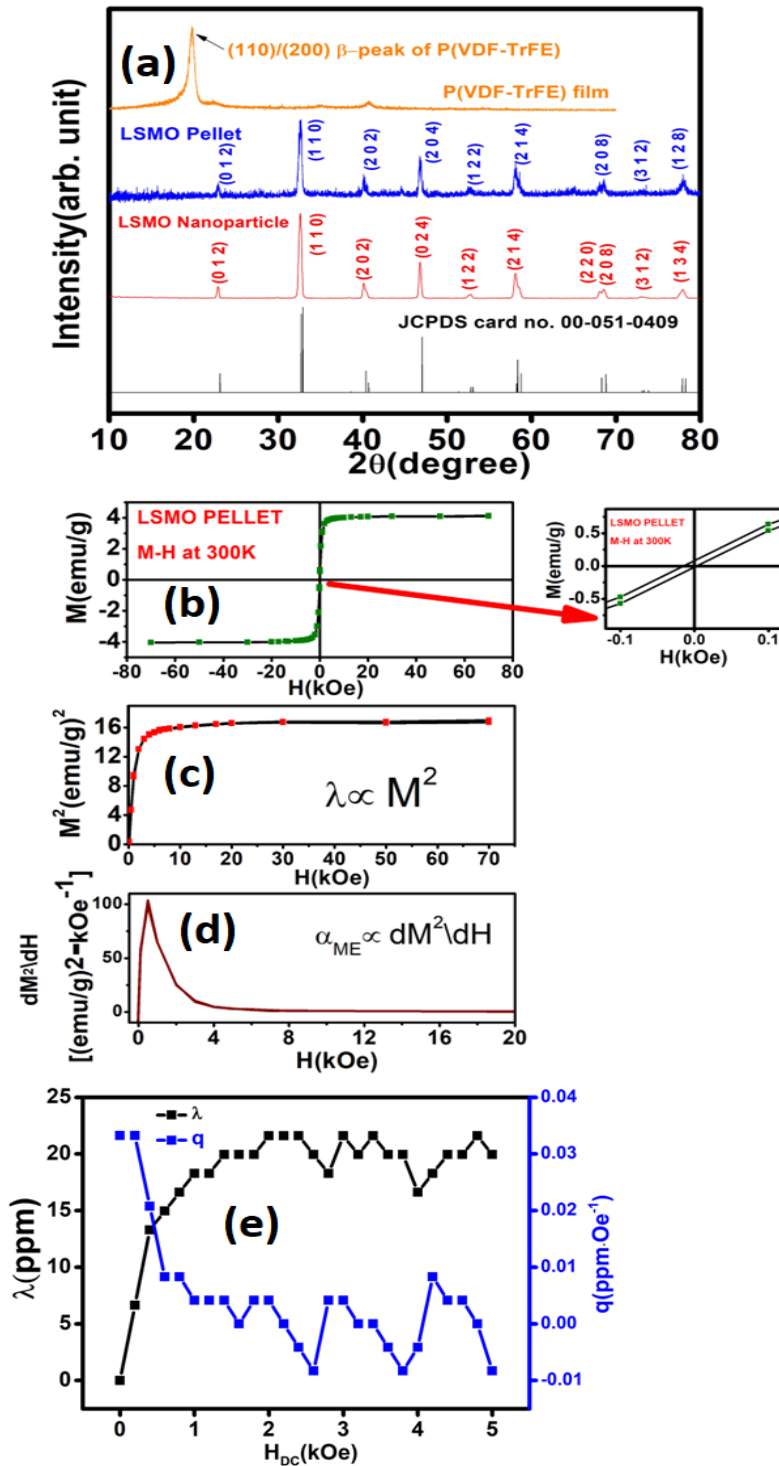


Figure 5. (a) Room temperature XRD pattern of the as casted P(VDF-TrFE) film, synthesized LSMO pellet and NPs along with the JCPDS pattern of LSMO NPs; (b) Room temperature M-H hysteresis curve, (c) M^2 -H variation of LSMO pellet, and (d) dM^2/dH Vs. H plot of LSMO Pellet; (e) Variation of in-plane magnetostriction (λ) and piezomagnetic coefficient (q) of LSMO pellet with applied magnetic field

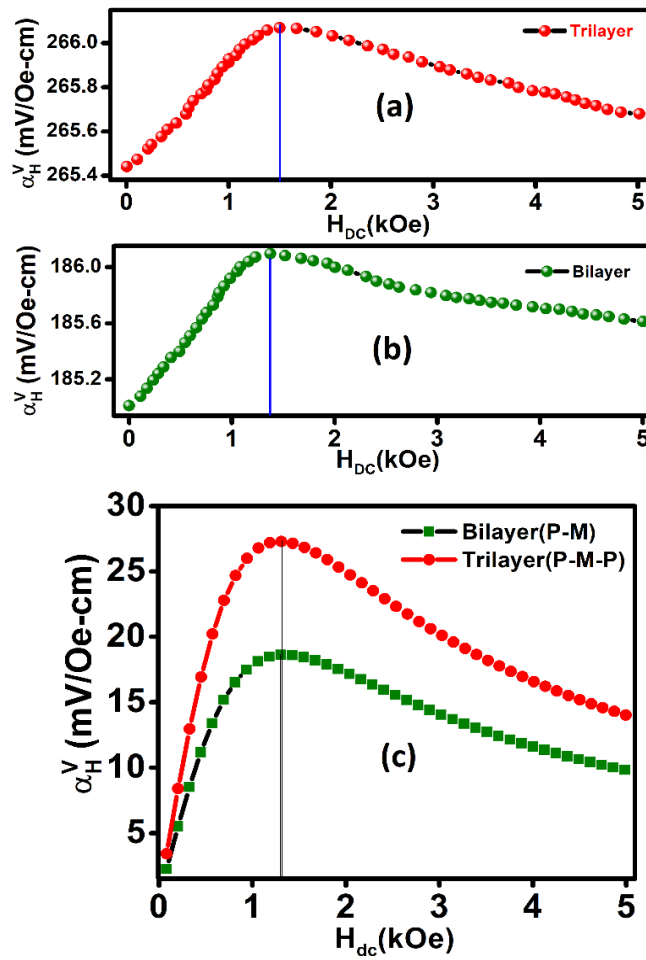


Figure 6. Plot of experimentally determined α_H^V with H for (a) tri-layer (P-M-P) and (b) bi-layer(P-M) LSMO/P(VDF-TrFE) laminate composites; (c) Plot of FEM based ME simulation results for variation of α_H^V with H by COMSOL Multiphysics 6.0 software for tri-layer (P-M-P) and bi-layer(P-M) LSMO/P(VDF-TrFE) laminate composites

Table 4. Experimental and simulated ME coefficient and bias field for bi-layer and tri-layer LSMO/P(VDF-TrFE) composite.

Sample	ME coefficient (Experimental) (mV/Oe-cm)	Bias field (Experimental) (kOe)	ME coefficient (Simulated) (mV/Oe-cm)	Bias field (Simulated) (kOe)
Bilayer or P-M structure	186.10	1.37	18.65	1.30
Tri-layer or P-M-P structure	266.07	1.49	27.34	1.31

4. CONCLUSION

ME effect in the (P-M) configured bilayer and P-M-P configured tri-layered or sandwiched structure of (2-2) LSMO/P(VDF-TrFE) laminated composites are explored both experimentally by lock-in technique and by finite element method (FEM) based simulation model in COMSOL Multiphysics 6.0 software. The experimental study on ME coupling coefficient reveals that “ α_H^V ”

is higher for tri-layer structure and the required bias magnetic field is also higher compared to bilayer structure. In the FEM based simulation, the magnetostrictive effect in LSMO layer was modelled by non-linear isotropic model whereas piezoelectric effect in P(VDF-TrFE) was modelled by linear constitutive equation of piezoelectricity. The nature of simulated results verify strain mediated ME effect and validate the experimental results obtained by the lock-in technique.

ACKNOWLEDGEMENT

This work was supported by Raja Ramanna Centre for Advanced Technology (RRCAT), Indore-452013 and Homi Bhabha National Institute (HBNI), Mumbai-400094. We want to acknowledge Dr. Rahul C. Kambale & Mr. Tulshidas C. Darvade of Savitribai Phule Pune University, Pune for the magnetostriction measurement.

REFERENCES

- [1] P. Martins & S. Mendez, (2013) "Polymer-Based Magnetolectric Materials", *Adv. Funct. Mater.*, Vol. 23, No. 27, pp3371-3385.
- [2] S. Koner, Sumit, R. Shukla, S. K. Majumder & S. Satapathy, (2022) "FEM modelling of magnetolectric coupling in (2-2) LSMO/ P(VDF-TrFE) polymer composite", *IOP Conf. Ser.: Mater. Sci. Eng.*, Vol. 1248, pp012079.
- [3] R. V. Demin, L. I. Koroleva & Y. M. Mokuvsii, (2005) "Giant volume magnetostriction and colossal magnetoresistance at room temperature in $\text{La}_{0.7}\text{Ba}_{0.3}\text{MnO}_3$ ", *J. Phys.: Condens. Mater.*, Vol. 17, No. 1, pp221-6.
- [4] R. V. Demin, L. I. Koroleva & A. M. Balbashov, (1998) "Anomalies of magnetostriction and thermal expansion in $\text{La}_{0.7}\text{Sr}_{0.3}\text{MnO}_3$ perovskite", *J. Magn. Magn. Mater.*, Vol. 177-181, No. 2, pp 871-872.
- [5] A. M. H. Gosnet & J. P. Renard, (2003) "CMR manganites: physics, thin films and devices", *J. Phys. D: Appl. Phys.*, Vol. 36, ppR127-R150.
- [6] A. P. Ramirez, (1997) "Colossal magnetoresistance", *J. Phys.: Cond. Mater.*, Vol. 9, pp8171-8199.
- [7] J. Stohr & H. C. Siegmann, Stanford, CA 2006, *Magnetism From Fundamentals to Nanoscale Dynamics*, Springer Publishers.
- [8] Z. F. Zi, Y.P. Sun, X. B. Zhu, Z. R. Yang, J. M. Dai & W. H. Song, (2009) "Synthesis of magnetoresistive $\text{La}_{0.7}\text{Sr}_{0.3}\text{MnO}_3$ nanoparticles by an improved chemical coprecipitation method", *J. Magn. Magn. Mater.*, Vol. 321, No. 15, pp2378-2381.
- [9] S. W. Ng, K.P. Lim, S. A. Halim, S. K. Chen & J. K. Wong, (2009) "Magnetoresistive and magnetic properties of $\text{La}_{0.67}\text{A}_{0.33}\text{MnO}_3$ (A= Ba, Ca, and Sr) prepared by co-precipitation method", *Solid State Sci. Technol.*, Vol. 17, No. 2, pp82-88.
- [10] S. Koner, P. Deshmukh, A. Ahlawat, A. Sagdeo, R. Singh, A. K. Karnal & S. Satapathy, (2021) "Effect of magnetic field on ferroelectric output voltage: a study on $\text{La}_{0.7}\text{Sr}_{0.3}\text{MnO}_3$ (LSMO)/P(VDF-TrFE) flexible multiferroic nanocomposite films", *J. Mater. Sci.: Mater. Electron.*, Vol. 32, pp21780-21797.
- [11] K. H. Cho, (2018) "Effect of Dimension Control of Piezoelectric Layer on the Performance of Magnetolectric Laminate Composite", *Korean J. Mater. Res.*, Vol. 28, No. 11, pp611-614.
- [12] M. Silva, S. Reis, C. S. Lehmann, P. Martin, S. L. Mendez, A. Lasheras, J. Gutierrez & J. M. Barandiaran, (2013) "Optimization of the Magnetolectric Response of Poly(vinylidene fluoride)/Epoxy/Vitrovac Laminates", *ACS Appl. Mater. Interfaces*, Vol. 5, No. 21, pp10912-10919.
- [13] D. Xavier, S. D. Kumar & V. Subramanian, (2022) "Significant magnetolectric coupling in P(VDF-TrFE)/48%NiFe bilayer laminate composite for energy harvesting applications", *J. Phys. D: Appl. Phys.*, Vol. 55, pp305502.
- [14] M. Sadeghi, Y. Hojjat & M. Khodaei, (2019) "Design, analysis, and optimization of a magnetolectric actuator using regression modeling, numerical simulation and metaheuristics algorithm", *J. Mater. Sci.: Mater. Electron.*, Vol. 30, pp16527-16538.

- [15] Z. Ren, L. Tang, J. Zhau, S. Zhang, C. Liu&H. Zhao, (2022)“Comparative study of energy harvesting performance of magnetoelectric composite-based piezoelectric beams subject to varying magnetic field”, Smart Mater. Struct.,Vol. 31, pp105001.
- [16] S. Koner, P. Deshmukh, A. A. Khan, A. Ahlawat, A. K. Karnal&S Satapathy,(2020)“Direction dependent strong magnetoelectric coupling in La_{0.7}Ba_{0.3}MnO₃ embedded poly(vinylidene fluoride-co-trifluoroethylene) flexible nano-composite films at room temperature”, Scr. Mater.,Vol.189, pp30-35.
- [17] S. Koner, P. Deshmukh, A. K. Karnal&S. Satapathy, (2022)“Angular dependent magnetoelectric effect of La_{0.7}Ba_{0.3}MnO₃(LBMO) embedded P(VDF-TrFE) particulate multiferroic nanocomposite”, J. Mater. Sci.: Mater. Electron., Vol.33,pp8534-8541.
- [18] P. P. J, V. R. Monaji, S. D. Kumar, V. Subramanian& D. Das, (2018)“Enhanced magnetoelectric response from lead-free (Ba_{0.85}Ca_{0.15})(Zr_{0.1}Ti_{0.9})O₃-CoFe₂O₄ laminate and particulate composites”, Ceram. Int., Vol. 44, pp4298-4306.
- [19] F. Fei, Z. C. Peng&Y. Wei, (2011)“Thickness effects on magnetoelectric coupling for Metglas/PZT/Metglas laminates”, Sci. China Phys. Mech. Astron., Vol. 54, No. 4,pp 581-585

AUTHORS

Mr. Sougata Koner is a PhD Scholar of Laser and Biomedical Applications Division (LBAD) of Raja Ramanna Centre for Advanced Technology(RRCAT), Indore-452013, Madhya Pradesh, India under the Homi Bhabha National Institute, Mumbai-400094, India. His research interests are in the magnetoelectric composite in particulate, laminate and thin film form along with the magnetoelectric effect-based energy harvesting applications.



Sumit is a PhD Research Scholar of Homi Bhabha National Institute, Mumbai, India and working at Synchrotrons Utilization Section at Raja Ramanna Centre for Advanced Technology, Indore, India. His research interest includes finite element analysis, piezoelectric materials, sensors and actuators, smart structures and devices, energy harvesting, optimization for engineering design, and deformable mirror for synchrotron radiation beamline. He received the MTech in mechanical engineering from Motilal Nehru National Institute of Technology, Allahabad, India in 2017.



Dr. Rahul Shukla is a Scientific Officer (SO-E)in Accelerator Physics and Synchrotrons Utilization Division,INDUS-2of Raja Ramanna Centre for Advanced Technology (RRCAT), Indore, India. He is also an Assistant Professor of Homi Bhabha National Institute (HBNI), Mumbai, India. His research disciplines are Materials Engineering, Mechanical Engineering and Engineering physics. His fields of expertise are Mechanical Engineering, Single crystal and Ferroelectrics.



Dr. Shovan Kumar Majumder is a Scientific Officer(SO-H) and Head of theLaser and Biomedical Applications Division (LBAD) of Raja Ramanna Centre for Advanced Technology (RRCAT), Indore-452013, Madhya Pradesh, India. He is also a Professor of Homi Bhabha National Institute (HBNI), Mumbai, India. His research areas are Biophotonics, Raman Spectroscopy, optical tweezers, phototherapy and nano-photonics.



Dr. Srinibas Satapathy is a Scientific Officer (SO-G) of theLaser and Biomedical Applications Division (LBAD) of Raja Ramanna Centre for Advanced Technology (RRCAT), Indore-452013, Madhya Pradesh, India& an Associate Professor of Homi Bhabha National Institute (HBNI), Mumbai, India. His research areas are Multiferroics, Magnetoelectric coupled composites, Device fabrication using Magnetoelectriccomposites, Nano phosphors for up conversion applications, Solar cell, Pyroelectric materials, Transparent ceramics, Nano materials for photonic applications and Up-conversion based nano materials for biological applications.

